# DEM Modeling: Lecture 06

## Introduction to Soft-Particle DEM Normal Contact Force Models. Part I

# Introduction to Soft-Particle DEM

- Most common type of DEM model
- Deterministic approach
- “Soft-particle” refers to the fact that particles can “deform” during a contact
  - particles remain geometrically rigid, “deformation” taken into account in force models
  - contact duration is finite
  - multiple contacts may occur simultaneously

# Introduction to Soft-Particle DEM…

- More flexible approach than hard-particle method
  - variety of force models and particle shapes
  - can model long lasting, multiple particle collisions as well as dilute systems
- Typically a more time consuming approach than hard-particle method
  - due primarily to small integration time steps
  - complex particle shapes can add to computational load

# Introduction to Soft-Particle DEM…

Start

Determine forces and torques acting on each particle in the system.

$$\mathbf{F}_{\text{net},i} = \sum \mathbf{F}_{\text{body},i} + \sum \mathbf{F}_{\text{surface},i}$$

$$\mathbf{T}_{\text{net},i} = \sum \mathbf{T}_{\text{body},i} + \sum \mathbf{T}_{\text{surface},i}$$

Use Newton's 2nd Law to determine each particle's acceleration.

$$m_i \ddot{\mathbf{x}}_i = \mathbf{F}_{\text{net},i}$$

$$I_{xx}\dot{\omega}_x + \left(I_{zz} - I_{yy}\right)\omega_y\omega_z = T_{\text{net},z}$$

$$I_{yy}\dot{\omega}_y + \left(I_{xx} - I_{zz}\right)\omega_x\omega_z = T_{\text{net},y}$$

$$I_{zz}\dot{\omega}_z + \left(I_{yy} - I_{xx}\right)\omega_x\omega_y = T_{\text{net},z}$$

Integrate in time to find the new particle states.

$$\dot{\mathbf{x}}_i = \int \ddot{\mathbf{x}}_i dt \qquad \dot{\mathbf{q}}_i = \mathbf{q}_i\left[0, \tfrac{1}{2}\boldsymbol{\omega}_i\right]$$

$$\mathbf{x}_i = \int \dot{\mathbf{x}}_i dt \qquad \mathbf{q}_i = \int \dot{\mathbf{q}}_i dt$$

End?

No.

Yes.

Stop.

# Soft-Particle Force Models

- Typical force models
  - weight
  - contact forces
  - cohesion (*e.g.* liquid bridging)
  - fluid forces

# Soft-Particle Force Models…

- Weight (gravitational body force)
  - acts at particle center of mass
  - does not cause a moment on the particle

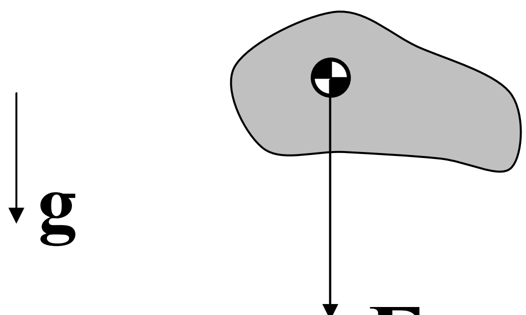


$$\mathbf{F}_i = m_i \mathbf{g}$$

$\mathbf{F}_i$ ≡ force acting on particle $i$
$m_i$ ≡ mass of particle $i$
$\mathbf{g}$ ≡ gravitational acceleration

# Soft-Particle Force Models…

- Contact forces
  - due to deformation of particle surfaces when particles are in contact
  - typically resolved into a normal force and a tangential force, with the normal force being independent of the tangential force

# Soft-Particle Force Models…

- In soft-particle DEM, particles are typically assumed to remain geometrically rigid during contact (e.g. spheres remain spheres) and "deformation" is accounted for in force models
  - DEM particles are allowed to overlap and the overlap characteristics (e.g. overlap or overlap volume) are used in determining the contact force
  - soft-particle DEM limited to <u>small deformations/overlaps</u>!

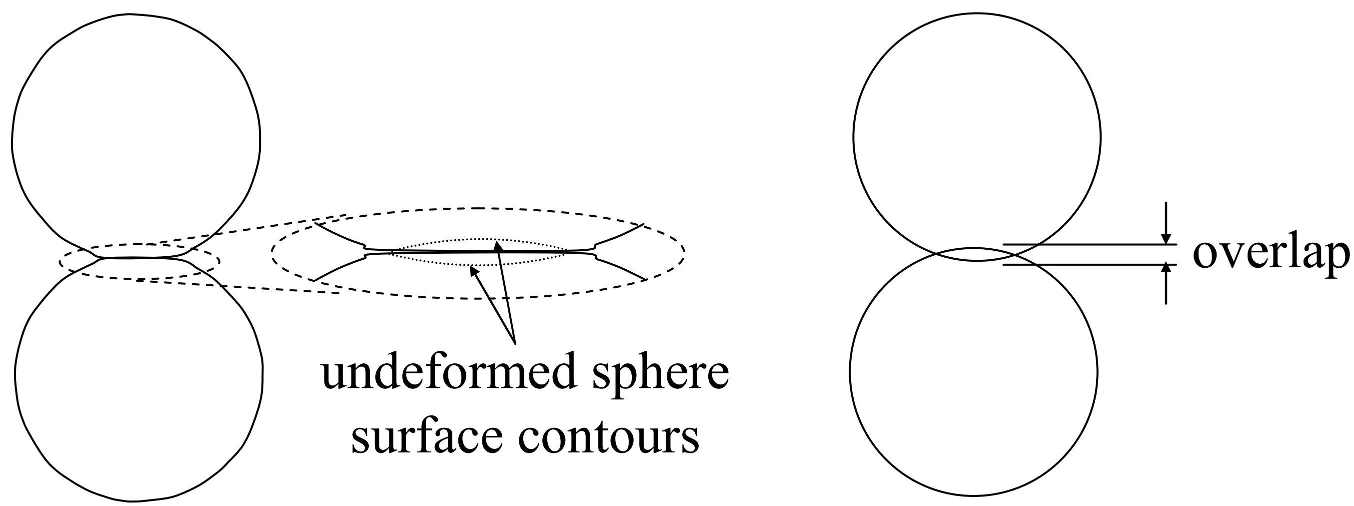

# Contact Kinematics

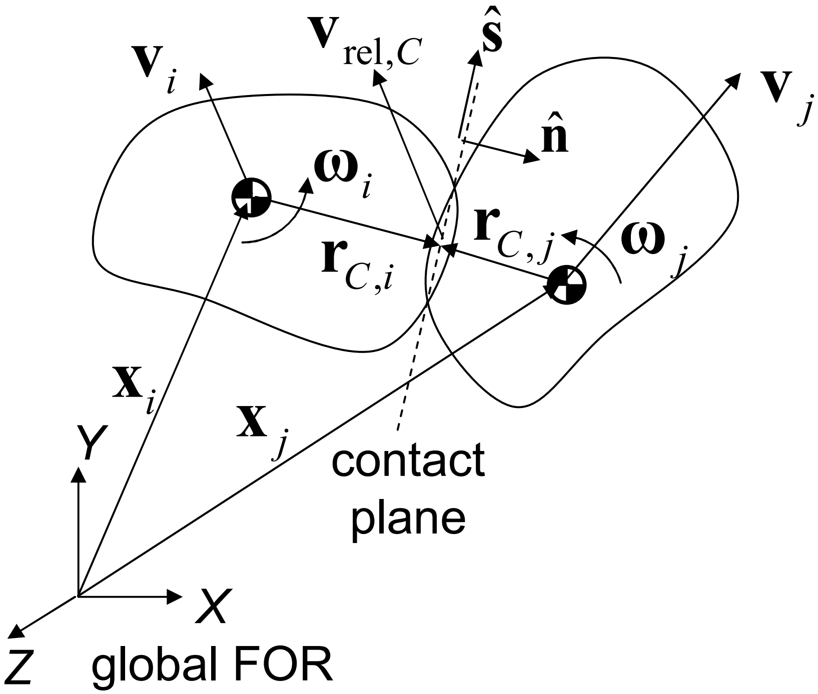


| | | |
|---|---|---|
| $\mathbf{x}$ | $\equiv$ | a particle's COM position |
| $\mathbf{v}$ | $\equiv$ | translational velocity of a particle's COM |
| $\boldsymbol{\omega}$ | $\equiv$ | angular velocity of a particle about its COM |
| $\mathbf{r}_C$ | $\equiv$ | position vector from a particle's COM to the point of contact |
| $\mathbf{v}_{\mathrm{rel},C}$ | $\equiv$ | velocity of particle *j* relative to particle *i* at the contact point |
| $\hat{\mathbf{n}}$ | $\equiv$ | unit vector normal to the contact plane and pointing from particle *i* toward particle *j* |
| $\hat{\mathbf{s}}$ | $\equiv$ | unit vector tangential to the contact plane and pointing in the direction of $\mathbf{v}_{\mathrm{rel},C}$ |

Note: Particle angular velocities are often given in a body-fixed frame of reference (FOR). All of the vectors shown above are assumed to be in a global FOR (including the particle angular velocities). A method for converting from a body-fixed to a global FOR will be presented in a future lecture.

# Contact Kinematics…

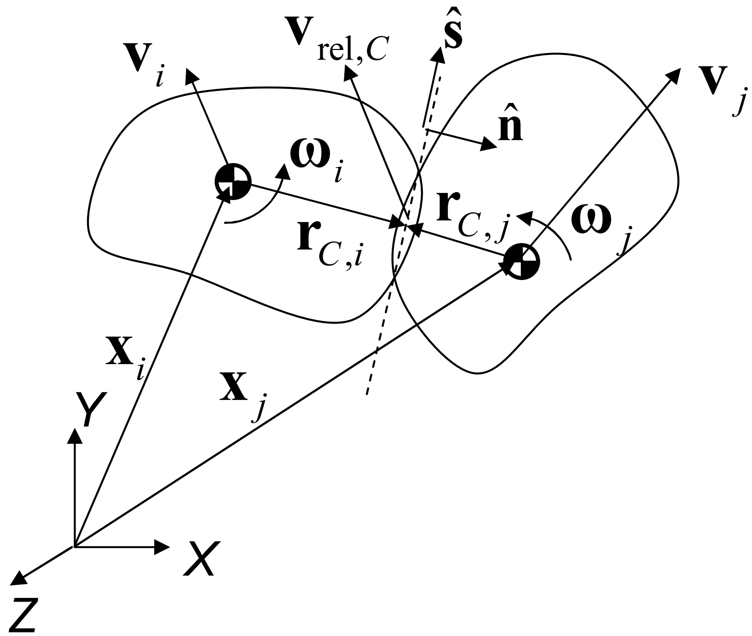


$$\mathbf{v}_{C,i} = \mathbf{v}_i + \boldsymbol{\omega}_i \times \mathbf{r}_{C,i}$$

$$\mathbf{v}_{C,j} = \mathbf{v}_j + \boldsymbol{\omega}_j \times \mathbf{r}_{C,j}$$

$$\mathbf{v}_{\mathrm{rel},C} = \mathbf{v}_{C,j} - \mathbf{v}_{C,i}$$

---

$$\mathbf{v}_{\mathrm{rel},C} = \left(\mathbf{v}_{\mathrm{rel},C} \cdot \hat{\mathbf{n}}\right)\hat{\mathbf{n}} + \left(\mathbf{v}_{\mathrm{rel},C} \cdot \hat{\mathbf{s}}\right)\hat{\mathbf{s}}$$

$$\Rightarrow \hat{\mathbf{s}} = \frac{\mathbf{v}_{\mathrm{rel},C} - \left(\mathbf{v}_{\mathrm{rel},C} \cdot \hat{\mathbf{n}}\right)\hat{\mathbf{n}}}{\left|\mathbf{v}_{\mathrm{rel},C} - \left(\mathbf{v}_{\mathrm{rel},C} \cdot \hat{\mathbf{n}}\right)\hat{\mathbf{n}}\right|}$$

---

$\dot{n}, \dot{s}$ $\equiv$ speed of particle *j* relative to particle *i* in the normal/tangential direction

$$\dot{n} = \mathbf{v}_{\mathrm{rel},C} \cdot \hat{\mathbf{n}}$$

$$\dot{s} = \mathbf{v}_{\mathrm{rel},C} \cdot \hat{\mathbf{s}}$$

# Contact Kinematics…

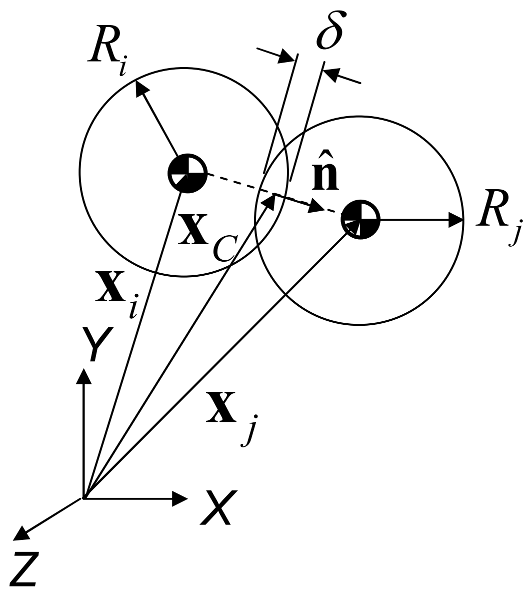


sphere/sphere contact:

$$\hat{\mathbf{n}} = \frac{\mathbf{x}_j - \mathbf{x}_i}{\left|\mathbf{x}_j - \mathbf{x}_i\right|}$$

$$\delta = \left(R_i + R_j\right) - \left|\mathbf{x}_j - \mathbf{x}_i\right| > 0$$

$$\mathbf{x}_C = \mathbf{x}_i + \left(R_i - \tfrac{1}{2}\delta\right)\hat{\mathbf{n}}$$

$$\mathbf{r}_{C,i} = \left(R_i - \tfrac{1}{2}\delta\right)\hat{\mathbf{n}}$$

$$\mathbf{r}_{C,j} = -\left(R_j - \tfrac{1}{2}\delta\right)\hat{\mathbf{n}}$$

$R$ ≡ radius of a sphere
$\delta$ ≡ normal contact overlap
$\mathbf{x}_C$ ≡ location of the contact point

# Normal Force Models

- Some normal contact force models
  - Hertzian spring
  - damped linear spring
  - hysteretic linear spring
  - damped, Hertzian spring
  - non-linear damped Hertzian spring
  - hysteretic, non-linear spring
  - continuous potential

# Hertzian Contact

- Elastic deformation of two concave, contacting objects

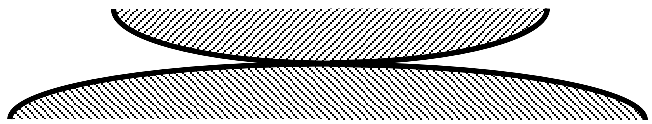

- First presented by Hertz (1882)
- Assumptions:
  - contact can be modeled using the linear theory of elasticity (*e.g.* continuous surfaces and no large strains)
  - the dimensions of the contact area are much smaller than the dimensions of the contacting bodies and the radii of curvature of the contacting surfaces
  - the contacting surfaces are frictionless

# Hertzian Contact…

- Hertzian contact between two spheres
  - refer to Johnson (1985) for the derivation
  - purely elastic contact, $\varepsilon_N = 1$

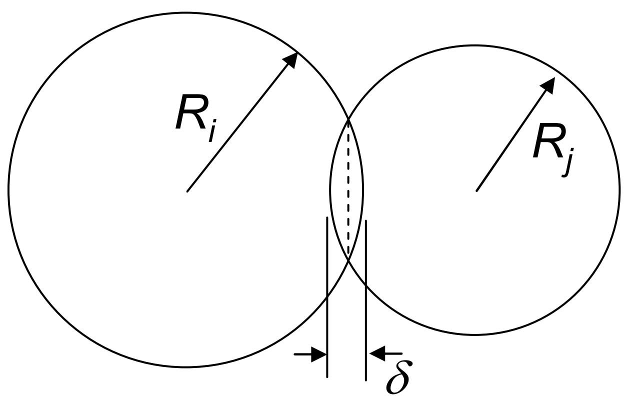


$$F = k_{Hz}\delta^{3/2}$$

$$k_{Hz} = \tfrac{4}{3} R'^{1/2} E'$$

$$\frac{1}{R'} = \frac{1}{R_i} + \frac{1}{R_j}$$

$$\frac{1}{E'} = \frac{1-\nu_i^2}{E_i} + \frac{1-\nu_j^2}{E_j}$$

$F$ ≡ force
$k_{Hz}$ ≡ Hertzian stiffness
$\delta$ ≡ overlap
$R'$ ≡ effective radius
$R_i$, $R_j$ ≡ radii of spheres *i* and *j*
$E'$ ≡ effective Young's modulus
$E_i$, $E_j$ ≡ Young's moduli for spheres *i* and *j*
$\nu_i$, $\nu_j$ ≡ Poisson's ratios for spheres *i* and *j*

# Hertzian Contact…

- **Consider two impacting particles**
  - **full derivation left as an exercise**

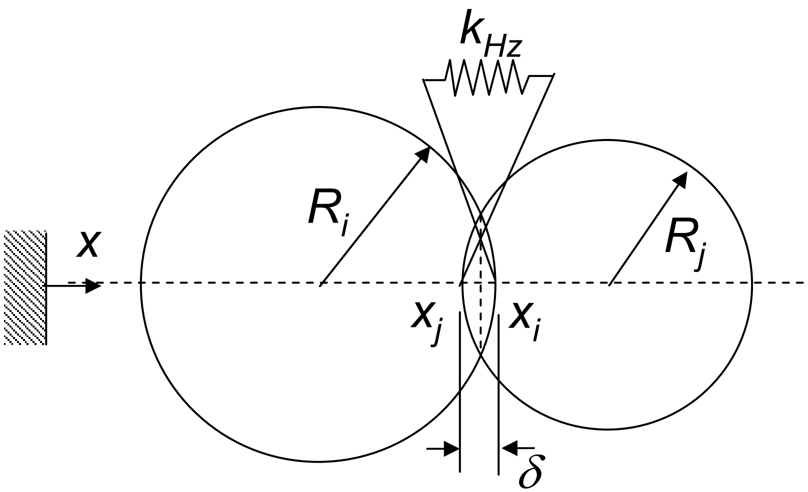


$$m_i \ddot{x}_i = F_i = -k_{Hz}\delta^{3/2}$$

$$m_j \ddot{x}_j = F_j = k_{Hz}\delta^{3/2}$$

$$\delta = x_i - x_j$$

$$\delta(t=0) = 0$$

$$\dot{\delta}(t=0) = \dot{\delta}_0$$

$$\boxed{\delta_{\max} = \left(\frac{15}{16}\frac{m'}{R'^{1/2}E'}\dot{\delta}_0^2\right)^{2/5}}$$

maximum overlap

$$\boxed{T \approx 2.870\left(\frac{m'^2}{R'E'^2\dot{\delta}_0}\right)^{1/5}}$$

contact duration

# Normal Force Trajectories

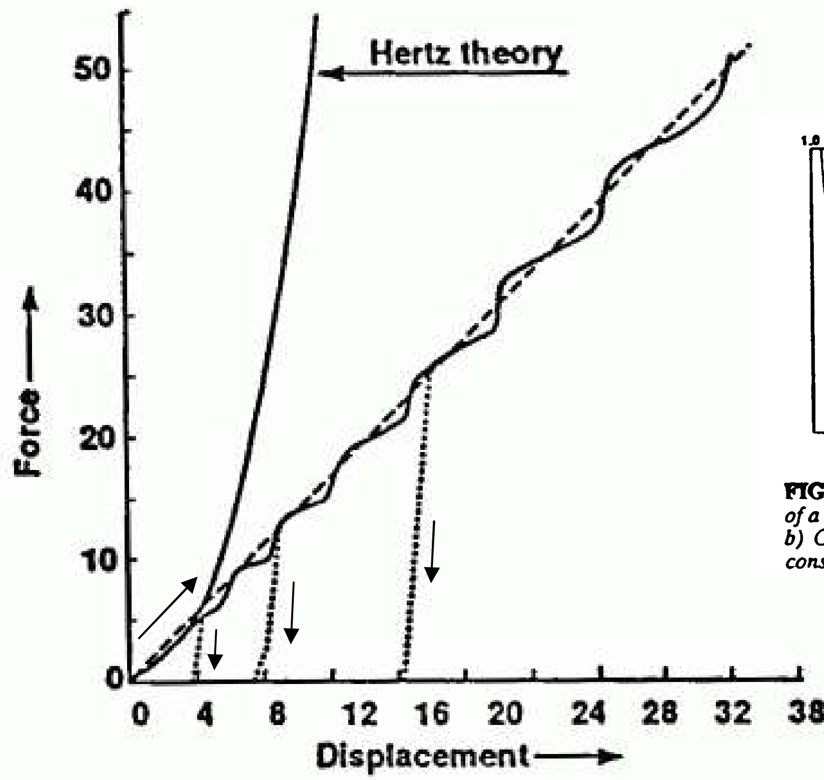


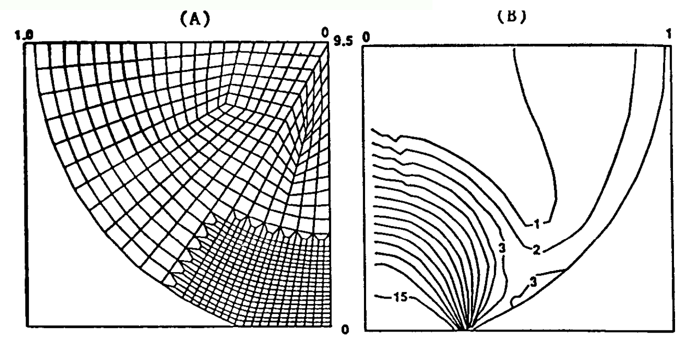


***FIGURE 25-4** a) Representative zoning used in finite element calculations of a hemisphere impinging on a rigid wall (Walton and Brandeis, 1984), and b) Calculated equal pressure contours using elastic-perfectly-plastic constitutive model.*

**FIGURE 25-5.** *Loading and unloading force-displacement behavior for elastic-plastic spheres during quasi static normal displacement as calculated using NIKE2D finite element model (Walton and Brandeis, 1984)*

From: Walton (1993)

# Normal Force Trajectories…

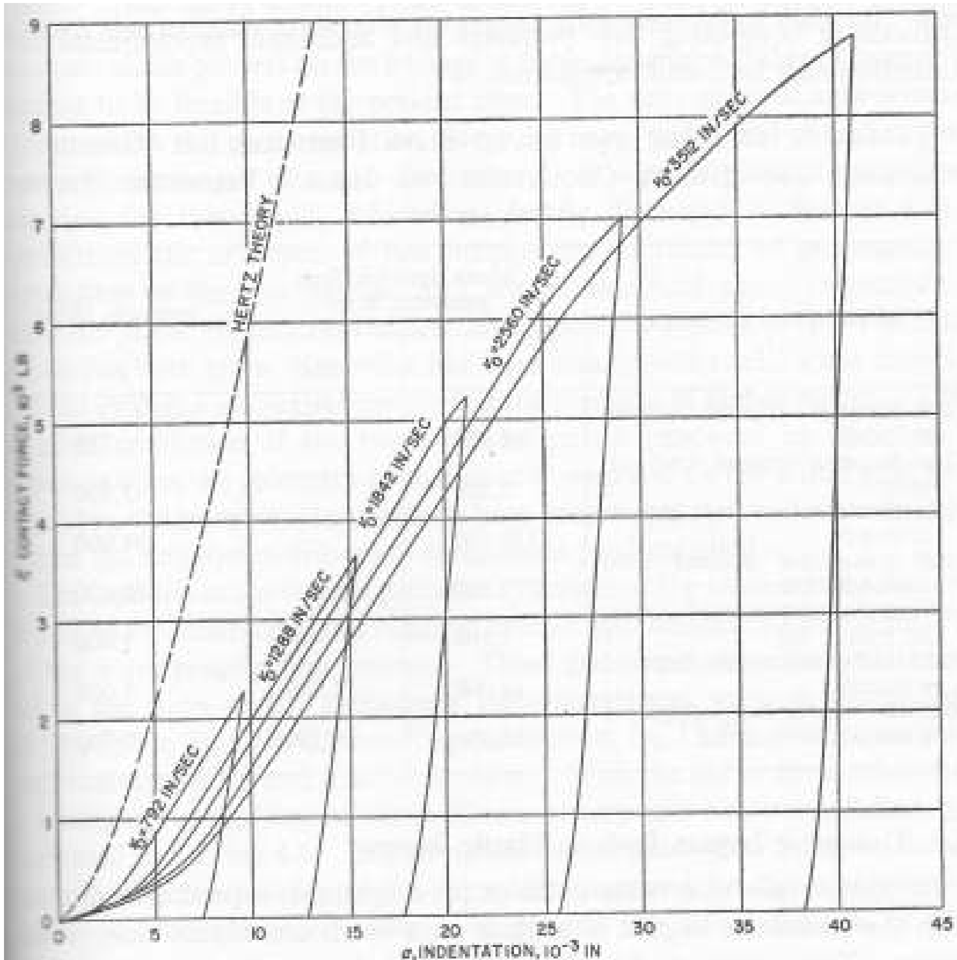


Figure 190. Force–Indentation Curves Derived from Data Obtained in Tests Involving the Longitudinal Impact of ½-in-diameter Steel Ball Bearings with the Plane End of a ½-in-diameter 2024 T4 Aluminium Rod at Various Initial Velocities

From Goldsmith (1960)

# Normal Force Trajectories…

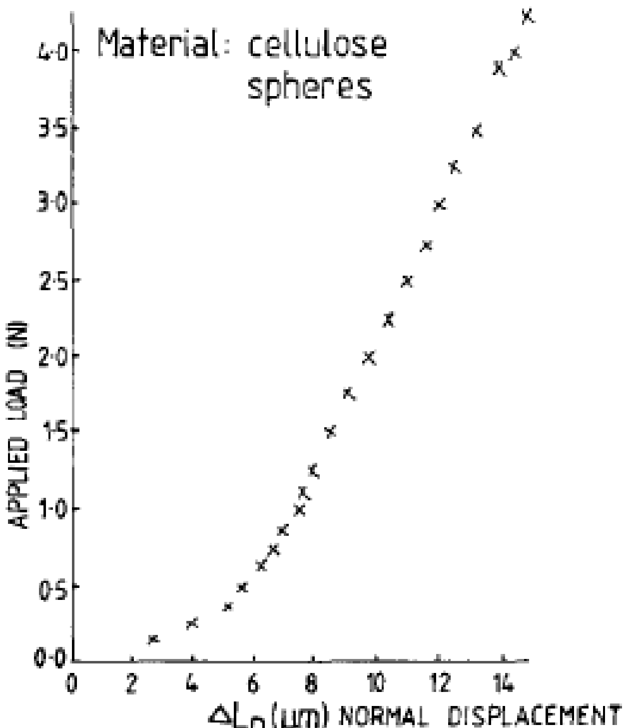


Fig. 11. Applied normal load *versus* normal displacement curve for cellulose acetate spheres.

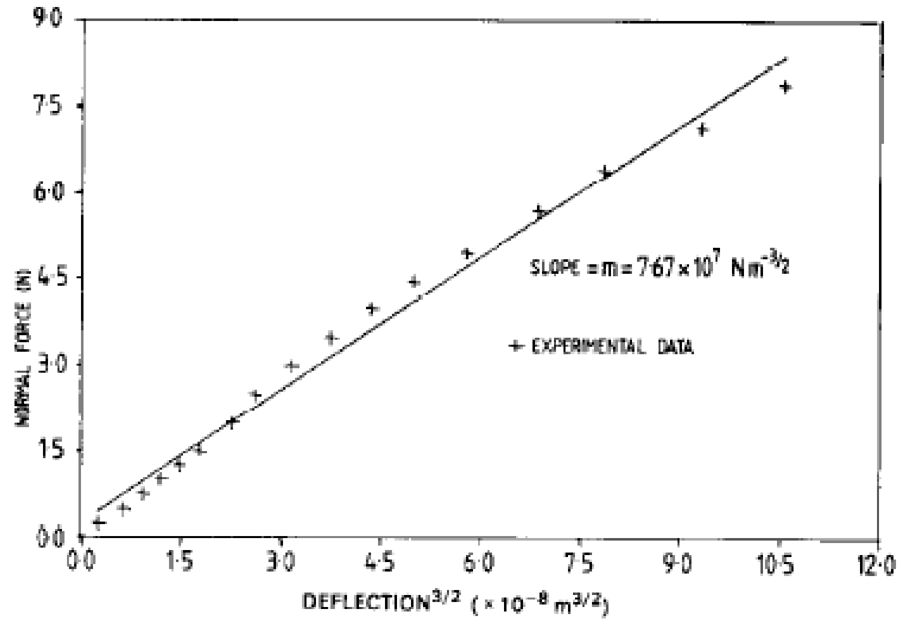


Fig. 14. Elasticity of normal force *versus* displacement response of cellulose acetate spheres.

Two 6 mm diameter cellulose acetate spheres

From Mullier *et al*. (1991)

# Elastic Wave Speed

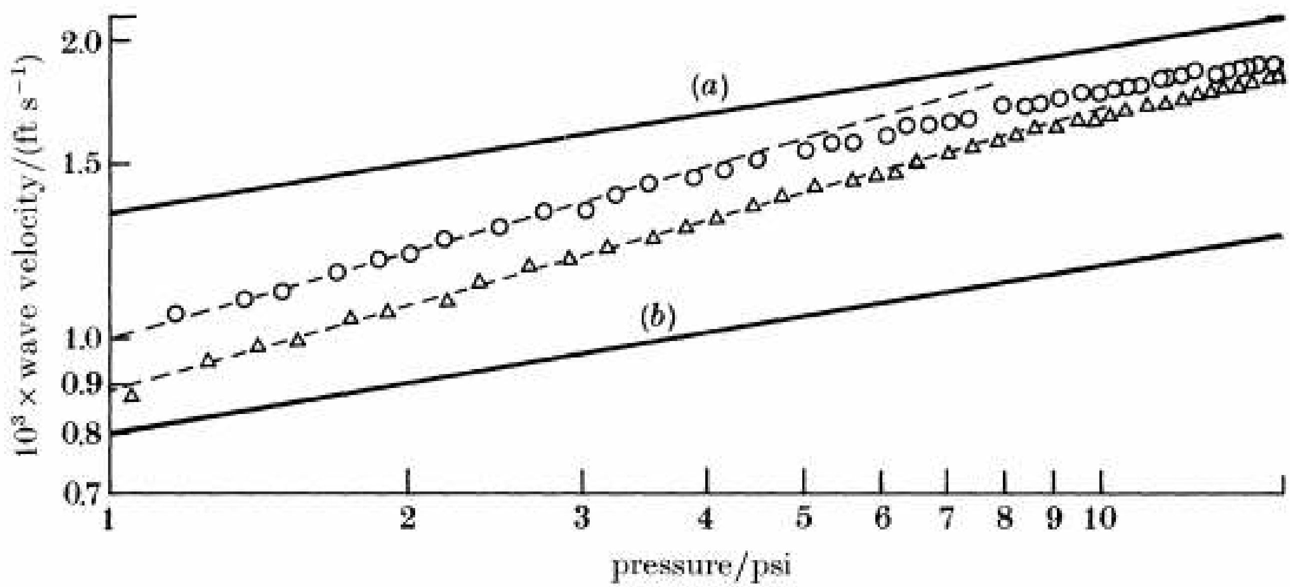


Figure 2. Elastic wave velocity in an FCC packing of $\frac{1}{8}$ inch diameter steel balls with 'low' (△) and 'high' (○) dimensional tolerances, $\pm 50 \times 10^{-6}$ inches and $\pm 10 \times 10^{-6}$ inches, respectively; after Duffy & Mindlin (1957), fig. 6 (first mode). Broken lines of slope $\frac{1}{4}$ have been added here. The solid lines with slope $\frac{1}{6}$ represent the Hertz–Mindlin contact, (*a*) with, and (*b*) without tangential stiffness. (1 psi $\approx$ 700 kg m$^{-2}$.)

Hertzian theory $\Rightarrow$ elastic wave speed $\propto p^{1/6}$
asperity (conical tip) contact $\Rightarrow$ elastic wave speed $\propto p^{1/4}$

From Goddard (1990)

# Normal Coefficient of Restitution…

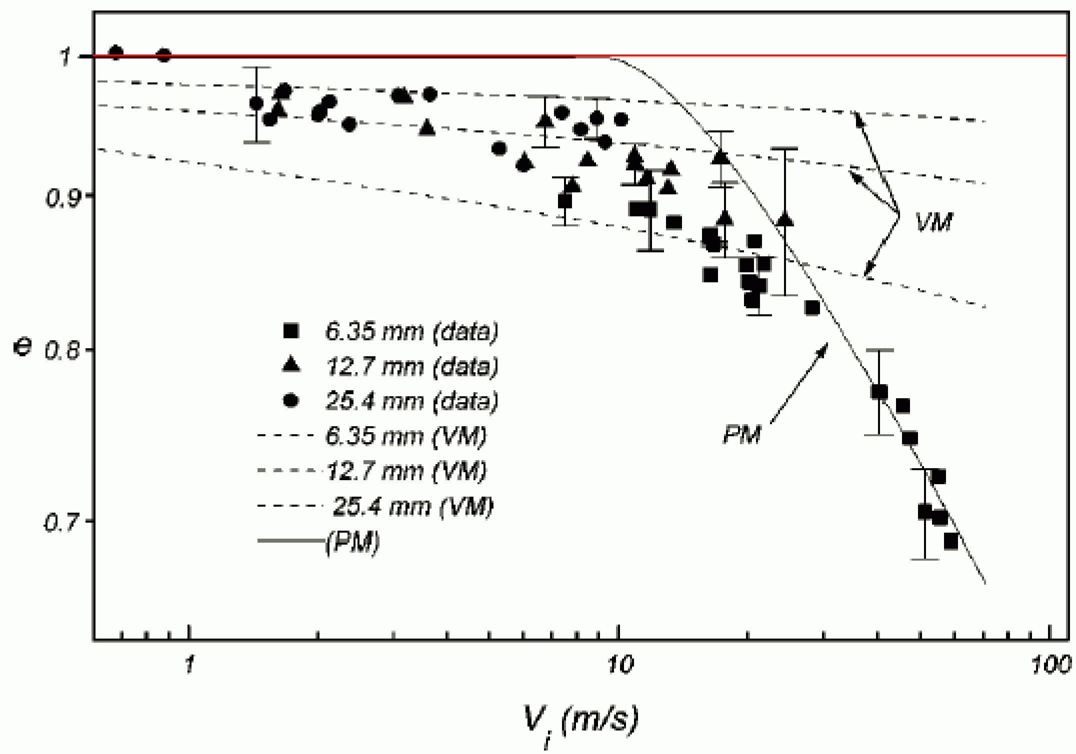


FIG. 7. Coefficient of restitution vs normal impact velocity for nylon spheres for different diameters on a log-log scale. The diameter of the spheres is shown in the figure. VM denotes the viscoelastic model. PM denotes plastic model.

**Hertzian contact**

plastic yield speed (Johnson, 1985):

$$v_{\text{yield}}^2 \approx 107 \frac{R'^3 Y^5}{m' E'^4}$$

VM: $1 - e \propto V^{1/5}$ ($e \to 1$)
PM: $e \propto V^{-1/4}$

(Kuwabara and Kono, 1987; Johnson, 1985)

From Labous *et al*. (1997)

# Contact Duration

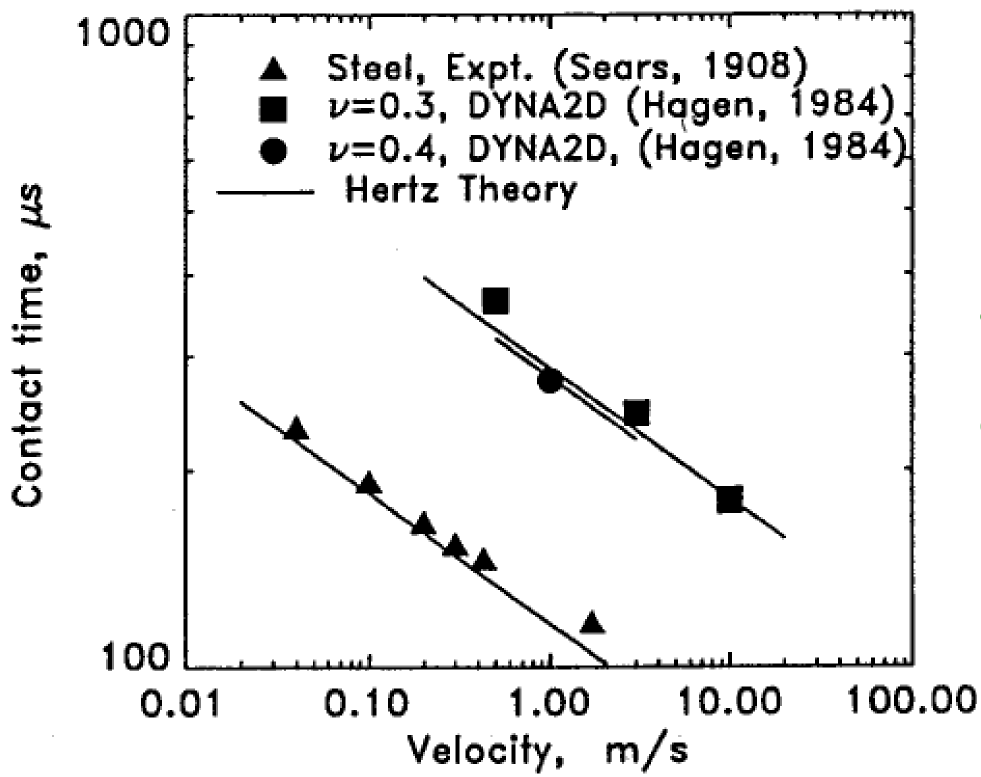


**FIGURE 25-2** *Calculated contact time for impacts of elastic spheres, (Walton and Hagen, 1984), and measured contact times, for impacts of rods with spherical ends (Sears, 1908), compared with Hertz theory predicted inverse 1/5 power dependence on incident velocity, solid lines.*

**Hertz theory is in good agreement with measured contact durations**

From Walton (1993)

# Contact Duration

- Difficult quantity to measure, usually use metallic particles

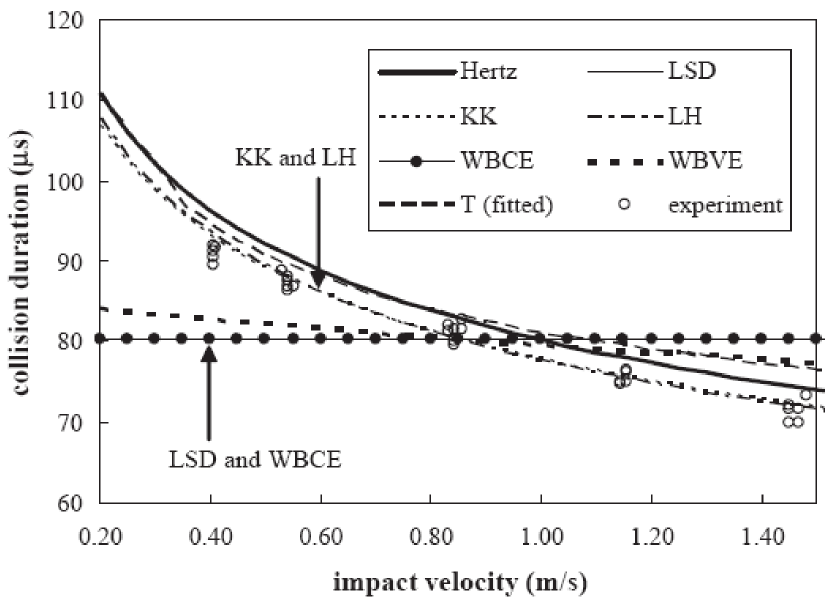


Fig. 4. Stainless steel system—comparison of experimental data and model predictions for collision duration. Simulation parameters are given in Table 2.

(stainless steel grade 316)

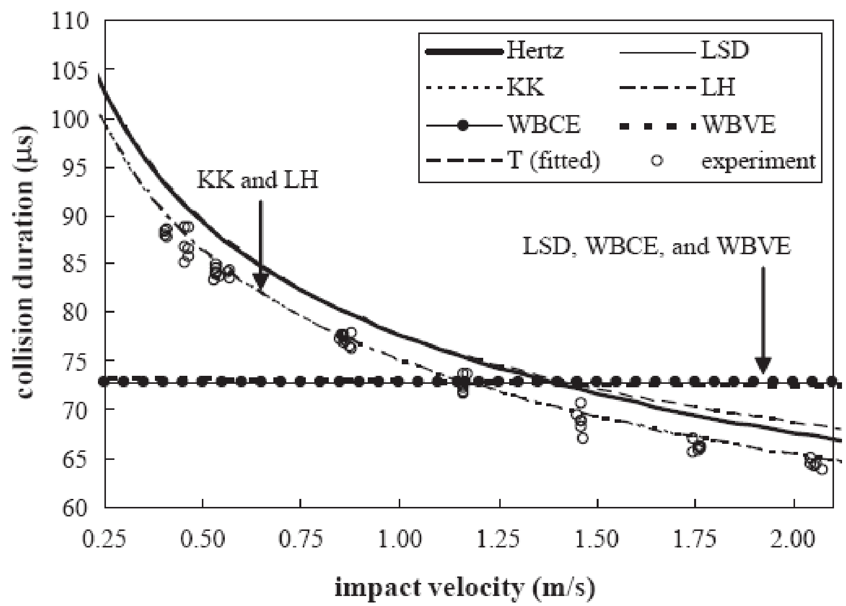


Fig. 9. Chrome steel system—comparison of experimental data and model predictions for collision duration. Simulation parameters are given in Table 2.

(chrome steel AISI 52100)

**Hertz theory is in good agreement with measured contact durations**

From Stevens and Hrenya (2005)

# Contact Duration…

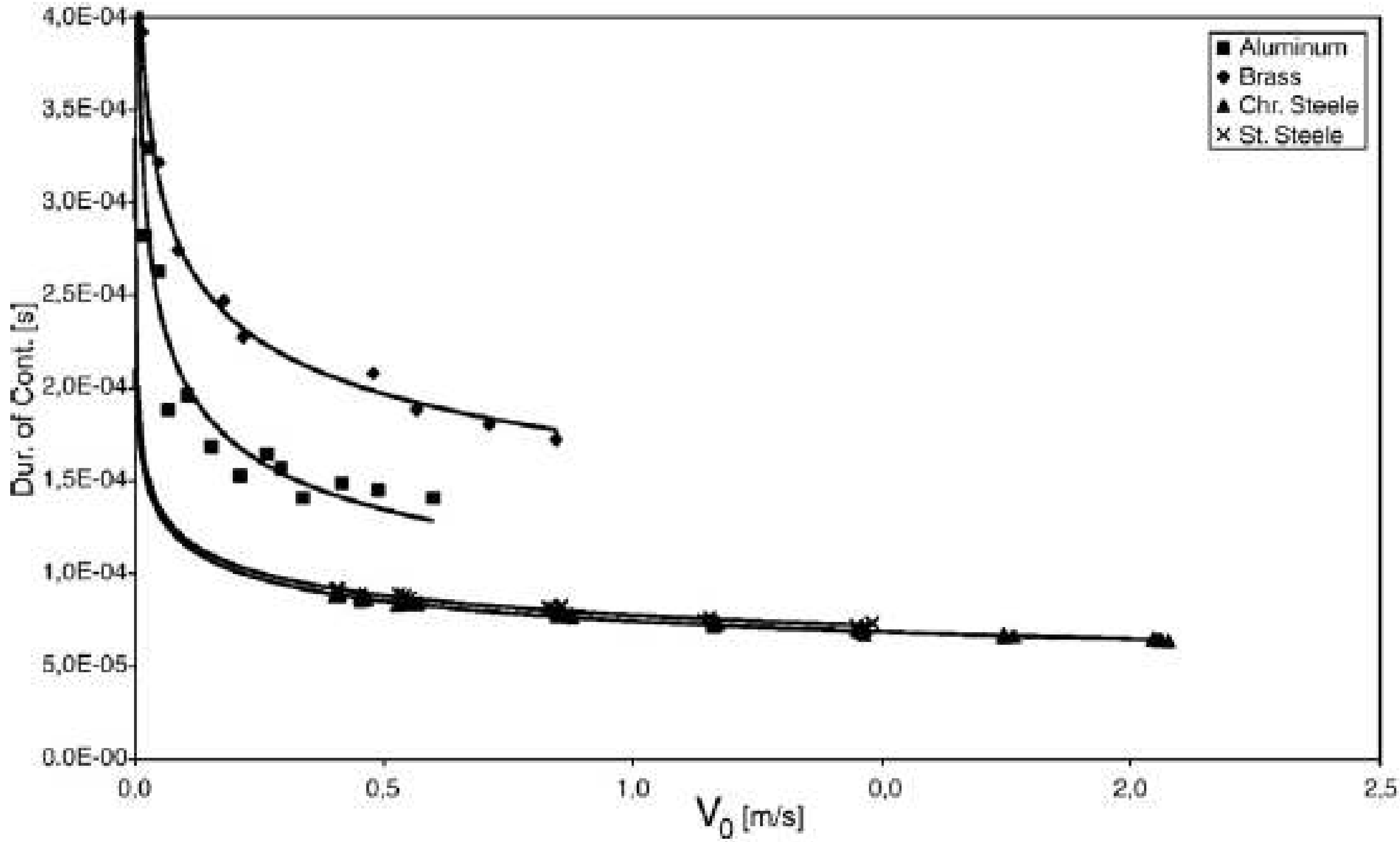


Fig. 4. Duration of contact as a function of the initial normal velocity $v_0$ [23,28].

From Kruggel-Emden *et al*. (2007)

# Hertzian Contact…

- Comments
  - full Hertzian force-displacement curve is considerably different than what is observed for real particles
  - Hertzian contact is elastic $\Rightarrow \varepsilon_N = 1$; real particles have $\varepsilon_N < 1$
  - contact duration is close to what is observed experimentally

# Normal Contact Force Model
# Damped Linear Spring

- First proposed by Cundall and Strack (1979)
- Widely used

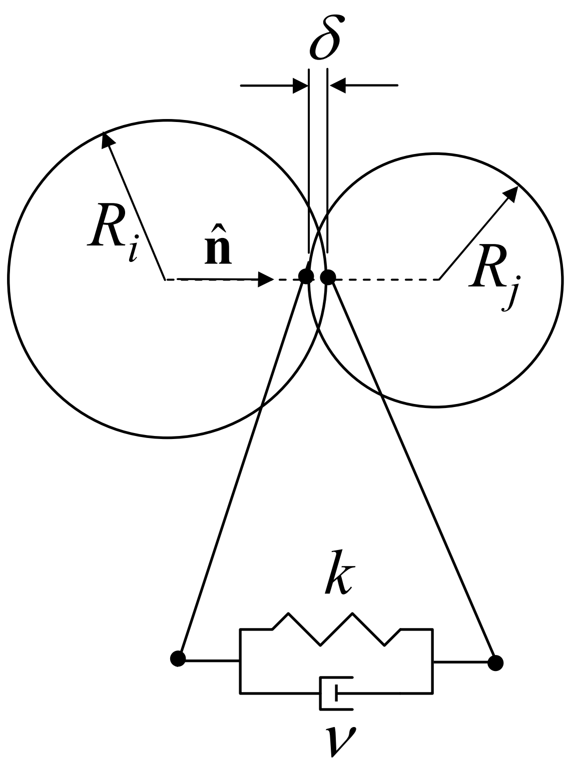


$$\mathbf{F}_i = \left(-k\delta + \nu\dot{\delta}\right)\hat{\mathbf{n}}$$

$k$ $\equiv$ spring stiffness
$\nu$ $\equiv$ damping coefficient

- damped linear spring aka Kelvin-Voigt element
- spring provides elastic rebound, dashpot dissipates energy
- contact force is discontinuous at start/end of contact due to damping force
- energy dissipation is velocity dependent
- simple model to implement

# Normal Contact Force Model Damped Linear Spring…

**For a two particle contact (derivation is left as an exercise):**

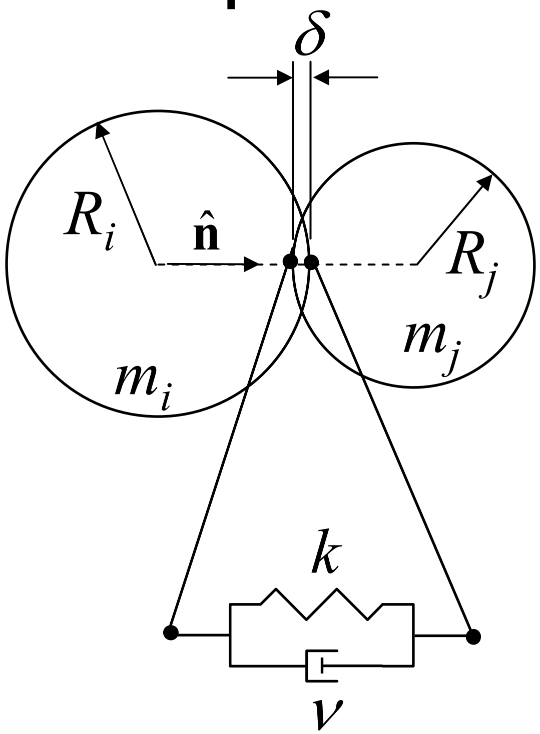


$$\nu = \sqrt{\frac{4m'k}{1+\beta^2}}$$

$$\delta_{\max} = \dot{\delta}_0 \sqrt{\frac{m'}{k}} \exp\left[ -\frac{\tan^{-1}(\beta)}{\beta} \right]$$

$$T = \pi \sqrt{\frac{m'}{k}\left(1+\frac{1}{\beta^2}\right)}$$

$\dot{\delta}_0$ ≡ relative impact speed
$m'$ ≡ effective mass (= $(m_i^{-1} + m_j^{-1})^{-1}$)
$\varepsilon_N$ ≡ normal coefficient of restitution
$T$ ≡ contact duration
$\beta$ ≡ $\pi/\ln(\varepsilon_N)$

Note: for $\varepsilon_N > 0.5 \Rightarrow$

$$\delta_{\max} \approx \tfrac{1}{2}(\varepsilon_N + 1)\dot{\delta}_0 \sqrt{\frac{m'}{k}} \quad (< \sim 1\% \text{ error})$$

$$T \approx \pi \sqrt{\frac{m'}{k}} \quad (< 3\% \text{ error})$$

# Normal Contact Force Model Damped Linear Spring…

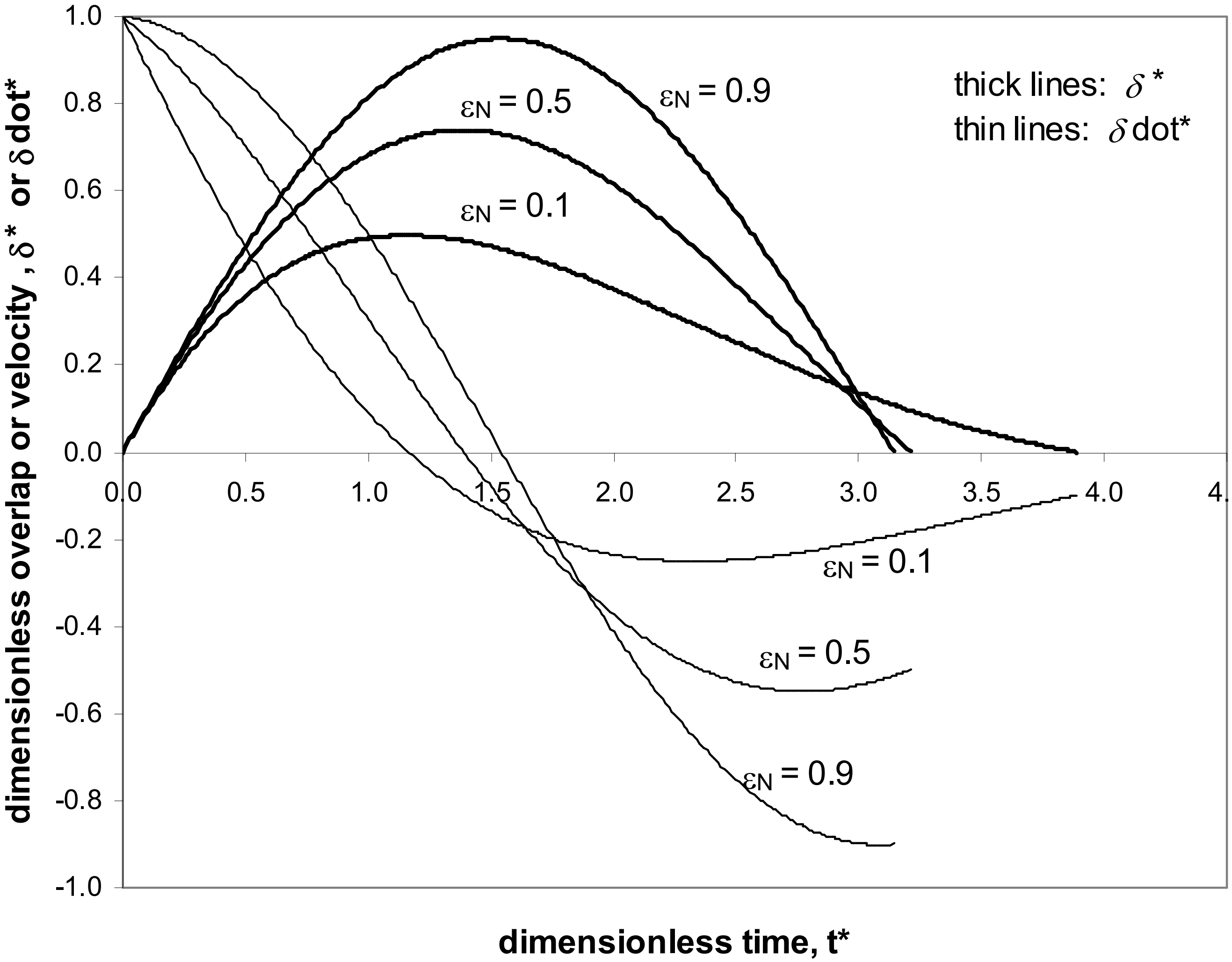


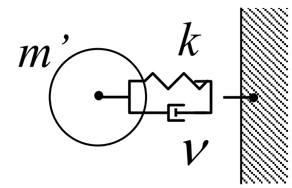


$$\delta^* \equiv \frac{\delta}{\dot{\delta}_0}\sqrt{\frac{k}{m'}}$$

$$\dot{\delta}^* \equiv \frac{\dot{\delta}}{\dot{\delta}_0}$$

$$t^* \equiv t\sqrt{\frac{k}{m'}}$$

# Normal Contact Force Model
# Damped Linear Spring…

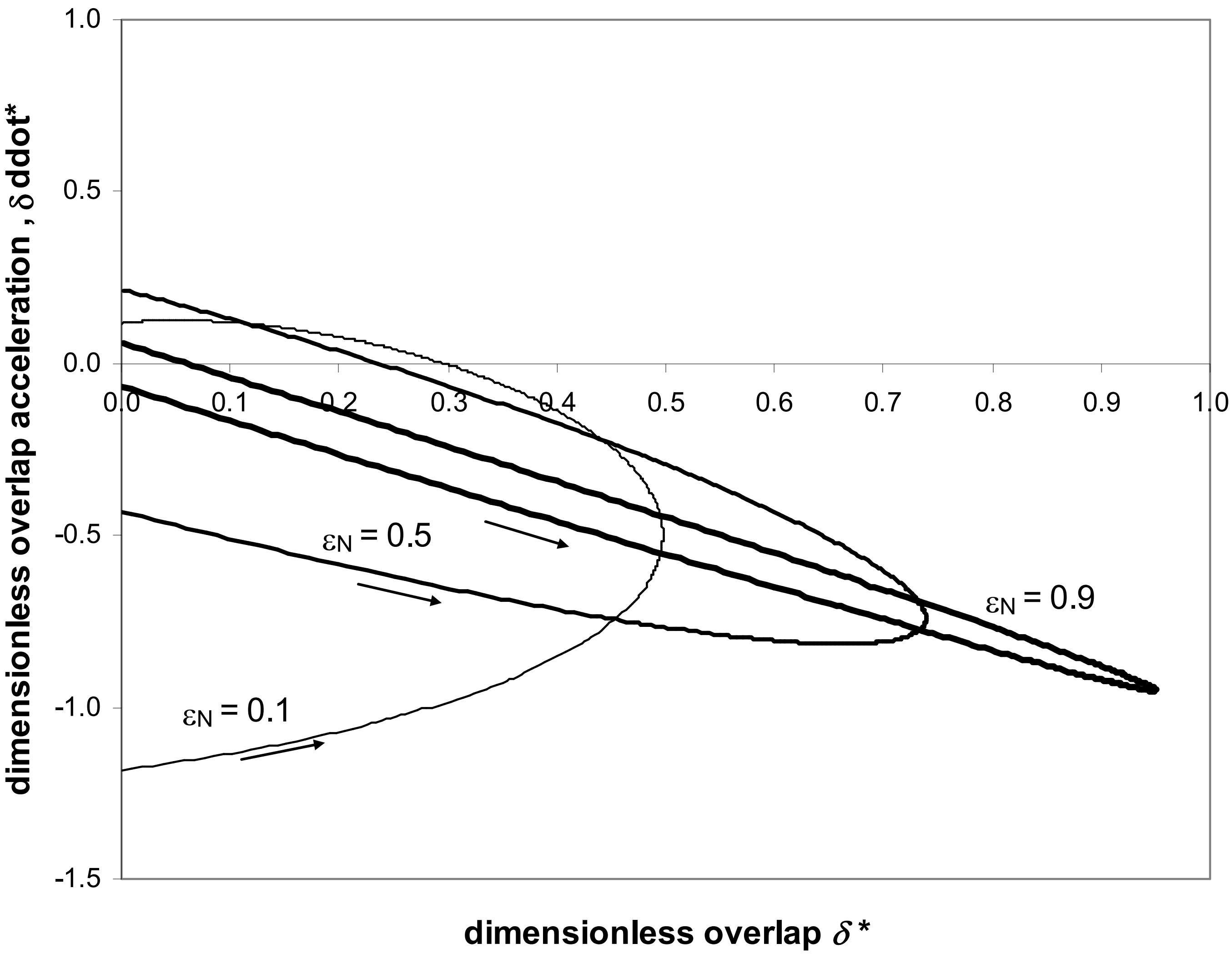


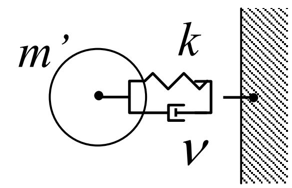


$$\ddot{\delta}^* \equiv \frac{\ddot{\delta}}{\dot{\delta}_0}\sqrt{\frac{m'}{k}}$$

$$\delta^* \equiv \frac{\delta}{\dot{\delta}_0}\sqrt{\frac{k}{m'}}$$

$$t^* \equiv t\sqrt{\frac{k}{m'}}$$

# Normal Contact Force Model Damped Linear Spring…

- Some observations
  - the contact force is discontinuous at the start and end of the contact due to the viscous damping force (real contact forces are continuous)
  - the contact force is cohesive toward the end of the impact (real contact forces are always repulsive for cohesionless systems)
  - energy dissipation is due to the damping force $\Rightarrow$ a function of the relative velocity between particles $\Rightarrow$ little energy loss for quasi-static systems
    - some researchers (e.g. Cundall and Strack, 1979) used global damping (a dashpot between a particle and the ground) to more quickly dissipate the energy – not very realistic

# Normal Contact Force Model Damped Linear Spring…

- Some observations…
  - coefficient of restitution is independent of impact speed (in real collisions $\varepsilon_N \downarrow$ as $\dot{\delta}_0 \uparrow$)
  - contact duration $\uparrow$ as $k \downarrow$, $m' \uparrow$, and $\varepsilon_N \downarrow$
    - larger contact durations are desirable since larger simulation integration time steps may be used (to be discussed in a future lecture)
    - contact duration is independent of impact speed (in real collisions, contact duration $\downarrow$ as impact speed $\uparrow$)
  - maximum overlap $\uparrow$ as $\dot{\delta}_0 \uparrow$, $m' \uparrow$, $k \downarrow$, and $\varepsilon_N \uparrow$
    - larger overlaps make the geometrically rigid particle assumption less accurate and can cause modeling errors due to excluded volume effects

# Normal Contact Force Model Damped Linear Spring…

- The dashpot coefficient ($\nu$) may be found from the spring stiffness ($k$) and the coefficient of restitution ($\varepsilon_N$):

$$\nu = \sqrt{\frac{4m'k}{1+\beta^2}} \quad \text{where} \quad \beta = \frac{\pi}{\ln \varepsilon_N}$$

- Method for determining the spring stiffness is not widely agreed upon
  - consider three methods, all of which set particular contact parameters equal to those found using a Hertzian contact model
    - maximum overlap
    - contact duration
    - maximum strain energy

# Normal Contact Force Model Damped Linear Spring…

– equivalent maximum overlap, $\delta_{\mathrm{max}}$

DLS model: $$\delta_{\max} = \dot{\delta}_0 \sqrt{\frac{m'}{k}} \exp\left[ -\frac{\tan^{-1}(\beta)}{\beta} \right]$$ where $\beta = \dfrac{\pi}{\ln \varepsilon_N}$

Hertzian spring model: $$\delta_{\max} = \left( \frac{15}{16} \frac{m'}{R'^{1/2} E'} \dot{\delta}_0^2 \right)^{2/5}$$

$$\boxed{\therefore k_{\mathrm{overlap}} \approx 1.053 \left( \dot{\delta}_0 m'^{1/2} R' E'^2 \right)^{2/5} \left\{ \exp\left[ -\frac{\tan^{-1}(\beta)}{\beta} \right] \right\}^2}$$

# Normal Contact Force Model Damped Linear Spring…

– equivalent contact duration, *T*

DLS model: $$T = \pi \sqrt{\frac{m'}{k}\left(1+\frac{1}{\beta^2}\right)}$$ where $\beta = \frac{\pi}{\ln \varepsilon_N}$

Hertzian spring model: $$T \approx 2.870\left(\frac{m'^2}{R'E'^2\dot{\delta}_0}\right)^{1/5}$$

$$\boxed{\therefore k_{\text{duration}} \approx 1.198\left(1+\frac{1}{\beta^2}\right)\left(\dot{\delta}_0 m'^{1/2} R'E'^2\right)^{2/5}}$$

# Normal Contact Force Model
# Damped Linear Spring…

– equivalent maximum strain energy, $SE_{max}$

DLS model: $SE_{\max} = \frac{1}{2} k \delta_{\max}^2$ where

Hertzian spring model: $SE_{\max} = \frac{2}{5} k_{Hz} \delta_{\max}^{5/2}$ where $k_{Hz} = \frac{4}{3} R'^{1/2} E'$

$$\delta_{\max} = \left( \frac{15}{16} \frac{m'}{R'^{1/2} E'} \dot{\delta}_0^2 \right)^{2/5}$$

$$\boxed{\therefore k_{L,\mathrm{SE}} \approx 1.053 \left( \dot{\delta}_0 m'^{1/2} R' E'^2 \right)^{2/5}}$$

# Normal Contact Force Model Damped Linear Spring…

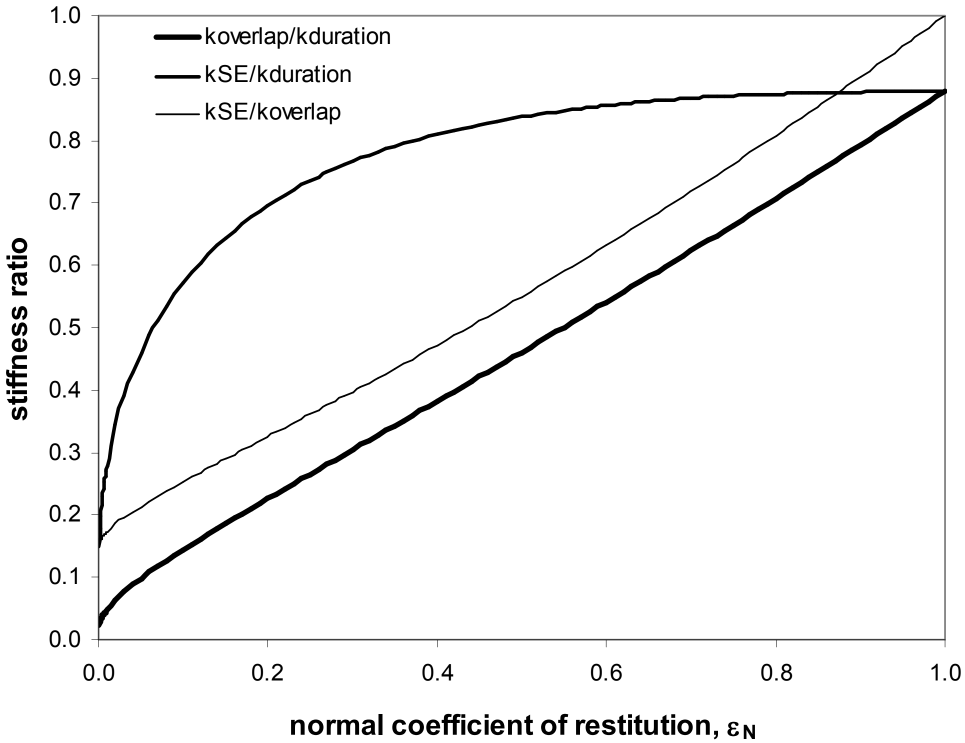


$$\frac{k_{\text{overlap}}}{k_{\text{duration}}} \approx \frac{k_{SE}}{k_{\text{duration}}} \left\{ \exp\left[ -\frac{\tan^{-1}(\beta)}{\beta} \right] \right\}^2$$

$$\frac{k_{SE}}{k_{\text{duration}}} \approx \frac{0.8788}{\left(1 + \frac{1}{\beta^2}\right)}$$

- For example: two 3.18 mm diam. soda lime glass spheres ($\rho$ = 2500 kg/m$^3$, $\nu$ = 0.22, $E$ = 71 GPa) impacting at 1 m/s ($\varepsilon_N$ = 0.97; Foerster *et al.*, 1994):
  - max overlap/eff. diameter = 0.2% $\Rightarrow$ $k_{\text{overlap}}$ = 1.96 MN/m
  - contact duration = 9.51 $\mu$s $\Rightarrow$ $k_{\text{duration}}$ = 2.29 MN/m
  - max strain energy = 10.5 $\mu$J $\Rightarrow$ $k_{SE}$ = 2.02 MN/m

# Normal Contact Force Model Stiffness Evaluation

- Which stiffness should be used?
  - limited overlap
    - Lan and Rosato (1997)
    - Corkum and Ting (1986)
    - Dury and Ristow (1997)
  - equivalent contact duration
    - Stevens and Hrenya (2005)
  - equivalent strain energy
    - Lan and Rosato (1995)
  - other methods
    - $k = k_{Hz}$: Buchholtz and Pöschel (1994)

# References


- Buchholtz, V. and Pöschel, T., 1994, “Numerical investigations of the evolution of sandpiles,” *Physica A*, Vol. 202, Nos. 3-4, pp. 390 – 401.
- Campbell, C.S., 2002, “Granular shear flows at the elastic limit,” *Journal of Fluid Mechanics*, Vol. 465, pp. 261 – 291.
- Corkum, B.T. and Ting, J.M., 1986, *The discrete element method in geotechnical engineering*, Publication 86-11, Department of Civil Engineering, University of Toronto, ISBN 0-7727-7086-7.
- Cundall, P.A. and Strack, O.D.L., 1979, “A discrete numerical model for granular assemblies,” *Géotechnique*, Vol. 29, No. 1, pp. 47 – 65.
- Dury, C.M. and Ristow, G.H., 1997, “Radial segregation in a two-dimensional rotating drum,” *Journal de Physique I*, Vol. 7, No. 5, pp. 737 – 745.
- Foerster, S.F., Louge, M.Y., Chang, H., and Allis, K., 1994, “Measurements of the collision properties of small spheres,” *Physics of Fluids*, Vol. 6, No. 3, pp. 1108 – 1115.
- Goddard, J.D., 1990, “Nonlinear elasticity and pressure-dependent wave speeds in granular media,” *Proceedings of the Royal Society London A: Mathematical and Physical Sciences*, Vol. 430, No. 1878, pp. 105 – 131.
- Goldsmith, W., 1960, *Impact: The Theory and Physical Behaviour of Colliding Solids*, Dover.
- Hertz, H., 1882, “Über die Berührung fester elastischer Körper,” *J. reine und angewandte Mathematik*, Vol. 92, pp. 156 – 171.
- Johnson, K.L., 1985, *Contact Mechanics*, Cambridge University Press.
- Ketterhagen, W.R., Curtis, J.S., and Wassgren, C.R., 2005, “Stress results from two-dimensional granular shear flow simulations,” *Physical Review E*, Vol. 71, Art. 061307.
- Kruggel-Emden, H., Simsek, E., Rickelt, S., Wirtz, S., and Scherer, V., 2007, “Review and extension of normal force models for the Discrete Element Method,” *Powder Technology*, Vol. 171, pp. 157 – 173.
- Kuwabara, G. and Kono, K., 1987, “Restitution coefficient in a collision between two spheres,” *Jpn. J.Appl. Phys.*, Vol. 26, pp. 1230 – 1233.
- Labous, L., Rosato, A.D., Dave, R.N., 1997, “Measurement of collisional properties of spheres using high-speed video analysis,” *Physical Review E*, Vol. 56, pp. 5717 – 5725.
- Lan, Y. and Rosato, A.D., 1995, “Macroscopic behavior of vibrating beds of smooth inelastic spheres,” *Physics of Fluids*, Vol. 7, No. 8, pp. 1818 – 1831.
- Lan, Y. and Rosato, A.D., 1997, “Convection related phenomena in granular dynamics simulations of vibrated beds,” *Physics of Fluids*, Vol. 9, No 12, pp. 3615 – 3624.
- Luding, S., Clément, E., Blumen, A., Rajchenback, J., and Duran, J., 1994, “Anomalous energy dissipation in molecular-dynamics simulation of grains: The detachment effect,” *Physical Review E*, Vol. 50, No. 5, pp. 4113 – 4124.
- Mullier, M., Tüzün, U., and Walton, O.R., 1991, “A single-particle friction cell for measuring contact frictional properties of granular materials,” *Powder Technology*, Vol. 65, pp. 61 – 74.
- Schäfer, J. and Wolf, D.E., 1995, “Bistability in simulated granular flow along corrugated walls,” *Physical Review E*, Vol. 51, No. 6, pp. 6154 – 6157.
- Stevens, A.B. and Hrenya, C.M., 2005, “Comparison of soft-sphere models to measurements of collision properties during normal impacts,” *Powder Technology*, Vol. 154, pp. 99 – 109.
- Walton, O.R., 1993, “Numerical simulation of inelastic, frictional particle-particle interactions,” in *Particulate Two-Phase Flow*, M.C. Roco, ed., Chap. 25, pp. 884 – 911, Butterworth-Heinemann.